Introduction

1.1 Introduction: Energy storage

To fulfill the growing and demanding energy requirements of the technologically evolving world, efficient, affordable and sustainable energy sources are always sought after. The new energy economy is redefining the need for worldwide transformation of energy dependence from the conventional fossil based resources to renewable sources [1]. The Department of Energy, US approved Bipartisan Infrastructure Law (BIL) in 2021 with an aim to widespread commercialization of advanced energy systems capable of delivering energy continuously for more than 10 hours [2]. The BIL supports energy storage via electrochemical, thermal and mechanical modes because these technologies have the capability to provide energy at reduced cost. It has also set an ambitious deadline for producing energy with net zero emission by 2050 and also lays down a roadmap to stabilize the global temperature and to fulfill other development related to sustainable energy. Similarly, the United Kingdom government announced the phasing out of fossil fuel driven automobiles by 2030 as part of their green industrial revaluation [3]. This certainly gives an impetus for electrification of transportation and, subsequently, demands development of energy efficient electric vehicles. This is possible with the advent of next generation low cost energy dense electrochemical energy storage devices namely batteries and supercapacitors. The applications of electrochemical energy storage devices are not only limited to electric vehicles but these devices also redefined and revamped the world of portable electronics.

A capacitor is a charge storage device that stores energy by separating positive and negative charges with the help of an electric field and releases energy in the form of electrical energy. These capacitors store energy at the electrode/electrolyte interface under applied electric field and thereby the process is capable of delivering energy at a faster rate but in small quantities since only the electrode surface takes part in the charge storage processes. The following chart compares the energy and power density of different energy storage devices which is popularly known as Ragone plot (Figure 1.1). It is always better to have an energy storage device with high energy and high power density. Specific energy is the parameter for capacitors and supercapacitors to work on for its implementations in practical applications. For that purpose, it is necessary to find suitable electrode materials and electrolytes.

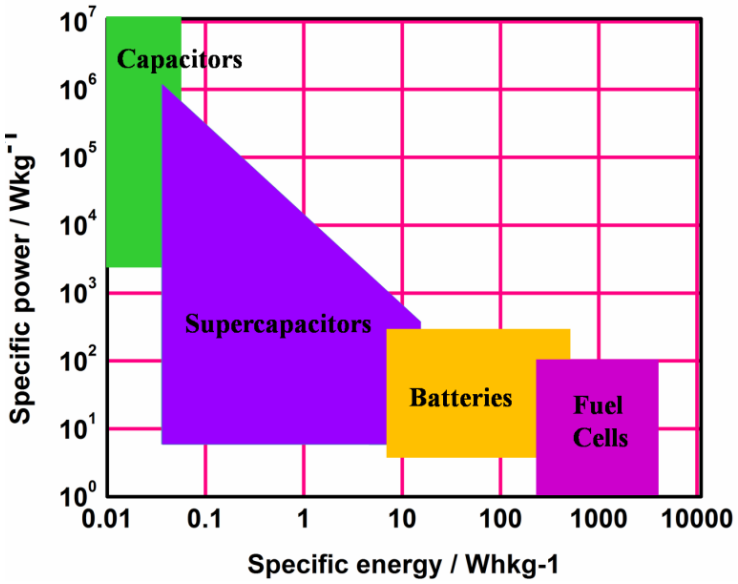

Figure 1.1: Ragone plot for different electrochemical energy storage devices

1.2 Supercapacitors

Supercapacitor is a subject of extensive study since the last two decades owing to their instant delivery of power in comparison to rechargeable batteries and ability to sustain millions of fast charge-discharge cycles [4-6]. In 1957, H. Becker for the first time discussed about supercapacitors in the patent titled "Low voltage electrolytic capacitor" [7]. Becker described the behavior of charges present at the electric double layer (EDL) capacitors at electrode/electrolyte interfaces and the principle of electrical energy storage of porous carbon material in an aqueous electrolyte. With the evolution of electronic devices during 1990s, the development of power sources with high energy as well as power density was essential to overcome the disadvantages of the conventional capacitors and knee-high power density of lithium-ion batteries [8-10]. To solve the issue, in the first approach, the conventional capacitor with high power density was combined with lithium-ion battery having high energy density. However, the process required additional accessories, thereby increasing the weight of the device and also resulting in the decrease in the energy density. During the same time, Conway's group introduced a different charge storage mechanism using RuO_2 films in H_2SO_4 electrolyte, which was termed as pseudocapacitance, associated with the electrochemical adsorption of charges with high specific capacitance and low internal resistance. However, the problem arose during the fabrication of capacitors at a large scale since RuO_2 is generally an expensive material.

The conventional capacitors are made up of two parallel metal plates separated by a dielectric like air, paper, ceramics, polyester etc. (Figure 1.2 a). The capacitance of traditional capacitors is in the range of microfarad. The supercpacitors are also a type of capacitor consisting of two current collectors with active material coated on it popularly known as cathode and anode which are separated by an electrolyte. The electrolyte can be either solid or liquid. Supercpacitors are categorized in three different groups based on their charge storage mechanisms: (i) electric double layer (EDL) capacitors where capacitance generated by the charges are accumulated at the electrode/electrolyte interfaces, (ii) pseudocapacitors, corresponding to fast reversible redox reaction, and (iii) hybrid supercapacitors. In hybrid supercapacitors, both physical and chemical processes are responsible for charge storage, and they are the evolved form of EDLC and pseudocapacitors to overcome various drawbacks of single mechanisms.

1.2.1 Electric Double Layer Capacitors (EDLC)

The concept of EDL capacitance was first explained by Becker in 1957, where he used a porous carbon material and an aqueous electrolyte. The double layer charge storage mechanism was first suggested by Helmholtz [11]. According to Helmholtz, oppositely charged ions accumulate at the electrode/electrolyte interfaces with a small separation depending on the size of the electrolyte's ions. These oppositely charged ions are developed near the electrode in the electrolyte to maintain the overall charge neutrality of the system by Coulombic interaction. Thus, the EDL is formed in between the electrode and electrolyte, as shown in Figure 1.2 b. The double layer structure proposed by Helmholtz is quite similar to that of the conventional capacitors. Considering the thermal motion of the ions and assuming charges to be point charge, Gouy and Chapman described another model for double layer formation. According to this model, the surface charge of the electrode is neutralized by the "diffuse layers" of oppositely charged ions due to the thermal fluctuation of the solution. Stern [12] modified Gouy and Chapman's model by considering the finite size of the ions. Both the Helmholtz and the diffusion layers were taken into account by Stern to calculate the total capacitance of the double layer. Grahame [13] further refined Stern's model by considering the size difference of the cations and anions (cations are smaller than the anions); hence, the cation and anion cover different distances from the electrode.

The parameters affecting the EDLC component of the double layer are as follows: size and concentration of the ions, ion-to-solvent interaction, specific absorption of the ions, and the solvent used as the electrolyte. The EDLC electrodes made up of porous carbon material with a very high specific surface area (~ 2000 m^2g^{-1}) and thin EDL give rise to an extremely high capacitance value. The pores in the porous carbon materials used in a supercapacitor electrode are categorized into three categories based on their size: (i) micropores (pore size < 2 nm), (ii) mesopores (2 ≤ poresize ≤ 50 nm), and (iii) macropores (pore size > 50 nm) [14]. Dynamics of the electrolyte ions in these pores significantly affect the specific capacitance of ES. If ES(1) and ES(2) are the surfaces of the two electrodes, C^+ and A^- are the cations and anions, respectively, and // represents the EDL, then the reversible charging/discharging process of EDLC can be explained as follows:

At the anode side:

$$ES(1) + A^- \rightleftarrows ES(1)^+//A^- + e^-$$

At the cathode side:

$$ES(2) + e^- + C^+ \rightleftarrows ES(2)^-//C^+$$

The overall charging and discharging reactions at the cathode and anode are as follows:

$$ES(1) + ES(2) + A^- + C^+ \rightleftarrows ES(1)^+//A^- + ES(2)^-//C^+$$

During charging, electrons flow from the anode to cathode by an external power, whereas in the electrolyte the cations move toward the cathode and the anions move towards the anode. The membrane present between the cathode and anode prevents a short circuit between them but allows the electrolyte ions to migrate from one side to another. As a result the cell voltage becomes very high and the energy is stored in the device.

During discharge, electrons flow from the cathode to anode and the stored energy is utilized. In EDLC process, electrodes do not undergo any structural and volumetric changes. Thus, these electrodes possess extremely high cycle life (~10^5 cycles). The supercapacitors following EDLC mechanism show high power density (> 500 Wkg^{-1}) owing to quick reversible charge storage-and-release processes at the electrode/electrolyte interfaces [15]. However, these physical charge transfer processes are confined only at the electrode surface, which results in low energy density of EDLC supercapacitors when compared to those of the batteries. Low energy density (< 10

$Whkg^{-1}$) is considered as one of the major drawbacks of the supercapacitors and this can be improved by using the pseudocapacitive charge storage mechanism.

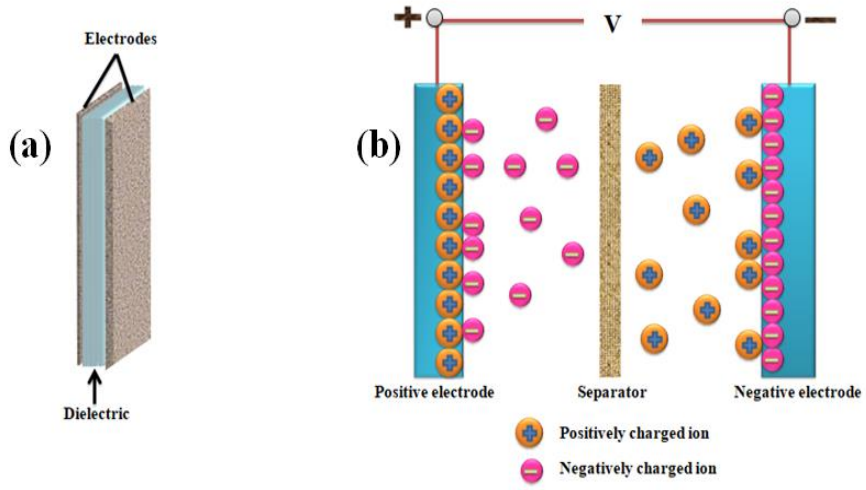

Figure 1.2: Schematic of (a) conventional capacitor, (b) charge storage in an electric double-layer capacitor (EDLC).

1.2.2 Pseudocapacitors

Pseudocapacitance is considered as the second mechanism to store charge in supercapacitors. In pseudocapacitive materials, fast charge transfer occurs by oxidation and reduction reactions at electrochemically active sites of the electrodes. The interaction of the charge carriers with the electrode material strongly influences the pseudocapacitive response of ESs. There are different types of pseudocapacitive processes contributing to the charge storage process such as redox adsorption of the ions from the electrolyte at the electrode surface and redox processes in the bulk provided the rate redox reaction is very fast. Pseudocapacitors possess much higher specific capacitance (10-100 times more) when compared to EDLC. The pseudocapacitive charge storage process utilizes both the outer surface and the available inner surface area in the bulk of solid electrode. The penetration of the electrolyte ions to the bulk of the electrode and the redox reactions in the electrode result in degradation of electrode materials which consequently lowers the cycling stability. Therefore, pseudocapacitors provide elevated specific capacitance at the cost of cycle life. Improving the cycle life of pseudocapacitive materials is the biggest challenge in the field of supercapacitors.

1.2.3 Hybrid Capacitors

In general, the energy density of EDLC is relatively low (< 10 $Whkg^{-1}$). Accordingly, to boost the energy density of EDLC up to 20-30 $Whkg^{-1}$, the concept of hybrid supercapacitor is introduced [16, 17]. Both EDLC and pseudocapacitance storage mechanisms have some advantages as well as drawbacks. The drawback of EDLC can be compensated by taking the advantages of pseudocapacitors and vice versa. The hybrid supercapacitors use electrode materials which exhibits both EDLC and pseudocapacitive charge storage mechanisms. The combination of both these mechanisms facilitates ESs with higher capacitive responses as compared to the conventional capacitors.

1.3 Battery

Batteries are basically classified into two categories: (i) primary battery and (ii) secondary battery. Primary batteries cannot be charged electrically and the redox processes associated with are irreversible in nature. On the other hand, the Faradic redox reactions involved in secondary batteries are reversible. Secondary batteries are also popularly known as rechargeable batteries. Hence, batteries can store relatively large amount of charges but the delivery process is slower than that of capacitors. This results in enhanced energy density but with lower power density. One of the primary objectives in the research field of rechargeable batteries is to develop electrode and electrolyte materials which can offer high energy and power density at an affordable rate of cost [18]. In the last three decades utmost emphasis on the research activities is given on rechargeable Li-ion batteries. It is needless to mention that these batteries have brought a paradigm shift in commercial energy storage platform because of extraordinary performance [19, 20]. The first Li-ion battery was fabricated with $LiCoO_2$ as cathode and graphitic-carbon as anode [21]. This is a remarkable invention which is offering best possible service to the mankind even today. But the use of Co-based electrode materials and the escalating demand for Li resources have made us to think for sustainable energy storage devices which can complement, if not replace, Li-ion batteries [22]. Hence, there is a spurt of research activities in battery chemistries which involve beyond Li-ion such as Na^+-ion, Mg^{2+}-ion, K^+-ion, Zn^{2+}-ion, Al^{3+}-ion etc.

Since the present thesis also discusses about Al^{3+}-ion electrochemistry, a brief discussion on Al-ion battery is given below.

1.3.1 Aluminum ion battery

As a beyond 'Li-ion' system, Al-ion batteries attracted significant attention recently. The interest in Al-ion batteries is sustained due to the following reasons: (i) metallic Al is easy to handle at ambient atmosphere, (ii) Al resources are less expensive, (iii) The three electron electrochemistry of Al is an attractive trait and (iv) Al has highest volumetric capacity (8056 $mAhcm^{-3}$) and better gravimetric capacity (2981 $mAhg^{-1}$) than that of Na (1166 $mAhg^{-1}$), Mg (2205 $mAhg^{-1}$), K (685 $mAhg^{-1}$), Zn (820 $mAhg^{-1}$) and Ca (1340 $mAhg^{-1}$). Highest volumetric capacity of aluminum implies higher energy storage per unit volume which consequently help in overall size reduction of the batteries. Few examples for Al-ion systems are discussed here. Holleck et al. investigated Al-ion battery with a vitreous carbon electrode utilizing $AlCl_3$-KCl-NaCl molten salt non-aqueous electrolyte [23, 24]. Archer et al. investigated Al-ion battery with V_2O_5 nanowires [25]. In this investigation, $AlCl_3$ and 1-methyl-3-ethylimidazolim chloride (MEICl) ionic liquid was used as an electrolyte. Lin et al. reported Al-ion battery with pyrolytic graphite/porous graphitic foam cathode in $AlCl_3$/1-ethyl-3-methylimidazolium chloride ionic liquid electrolyte in the year 2015 [26]. This Al/graphite cell could deliver high power density of 3000 Wkg^{-1} and sustained for more than 7500 cycles without any capacity decay.

1.3.2 Aqueous electrolytes

The commercially available Li-ion batteries generally use non-aqueous electrolytes. These electrolytes are however highly flammable and expensive. As an alternative, aqueous electrolytes for batteries may be promising although there are certain limitations such as small electrochemical stability window. Nonetheless, aqueous batteries are gaining research interest in recent times. The first demonstration of aqueous Li-ion cell was shown by the group of Jeff Dahn [27]. Some advantages can be reaped off from aqueous electrolytes such as: (i) safety issue could be mitigated during thermal run-away (ii) reduction in cost, (iii) aqueous electrolytes are less hazardous than organic solvents based non-aqueous electrolytes.

Most of the studies on Al-ion systems were performed using choloroaluminate ionic liquid based electrolytes. Although some of the studies show remarkable performance, there are certain demerits of this electrolyte such as high corrosion, high cost, and degradation in ambient atmosphere etc. Therefore, aqueous electrolytes in Al-

system may also be interesting. There are few reports on aqueous Al-ion systems available and these are discussed here. The concept of aqueous rechargeable Al-ion batteries is recent and was introduced in the year of 2015 by Liu et al. using TiO_2 as anode with $Al_2(SO_4)_3$ electrolyte [28]. Al-ion electrochemistry has been widely investigated for different morphology of TiO_2 in aqueous $AlCl_3$ electrolyte [29-31]. Liu et al. reported Al^{3+}-ion electrochemistry for TiO_2 nanotube arrays using aqueous $AlCl_3$ electrolyte and obtained 75 $mAhg^{-1}$ of discharge capacity. Also, Kazazi et al. investigated aluminum ion battery for TiO_2 nanospheres and reported capacity of 180 $mAhg^{-1}$. Lahan et al. investigated reversible Al^{3+}-ion inertion/ extraction in graphen/TiO_2composite [32]. They reported the enhanced diffusion coefficient after incorporation of graphene. Also, Lahan et al. reported Al^{3+} ion electrochemistry of MoO_3 for different Al^{3+} based electrolytes [33]. The report demonstrated $AlCl_3$ as better electrolyte than $Al_2(SO_4)_3$ and $Al(NO_3)_3$ for MoO_3 for better storage capacity and stability. Lahan et al. also investigated the possibility of Al^{3+}-ion intercalation/ extraction for WO_3 [34].

The present thesis could be categorized in two parts. In the first part, electrochemical investigations on nanocomposites of conducting polymers, 2D materials such as graphene/MoS_2 are illustrated for supercapacitor. The second part describes the complex Al^{3+}-ion electrochemistry in exfoliated MAX phase and $LiFePO_4$. Therefore, a brief description of these electrode materials is given below.

1.4 Conducting Polymers

Conducting polymers are considered as supercapacitor electrode material because of their high storage capacity, high conductivity when doped, high potential window, high energy density, environment-friendliness, low cost, and easy synthesis [35, 36]. Conducting polymers show rapid doping and de-doping process during faradic charge transfer process. Oxidation and reduction processes in the conducting polymer backbone can generate delocalized "π" electrons, and the electronic states of the π electrons determine the potentials of these states.

Polyaniline (PANI) is the most extensively used conducting polymer for supercapacitors owing to high specific capacitance in acidic media, high electroactivity, good environmental stability, high doping level, and highly conducting matrix [37, 38]. Depending upon the synthesis process, morphology, and thickness of the film, PANI

exhibits wide range of capacitance from 400 to 500 Fg^{-1} in aqueous acidic medium [39]. Electrochemically deposited PANI shows higher specific capacitance than chemically synthesized due to the homogeneous distribution in electrochemical polymerization. Li-doped PANI possesses cycling stability of 70% after 5000 cycles [40]. Polypyrrole (PPy) is famous among the conducting polymers for energy storage application owing to its high flexibility and easy synthesis [41]. The greater density of PPy minimizes the capacitive response of the polymer in thick coating electrodes due to the limited access of the electrolyte ions ascribed to high density.

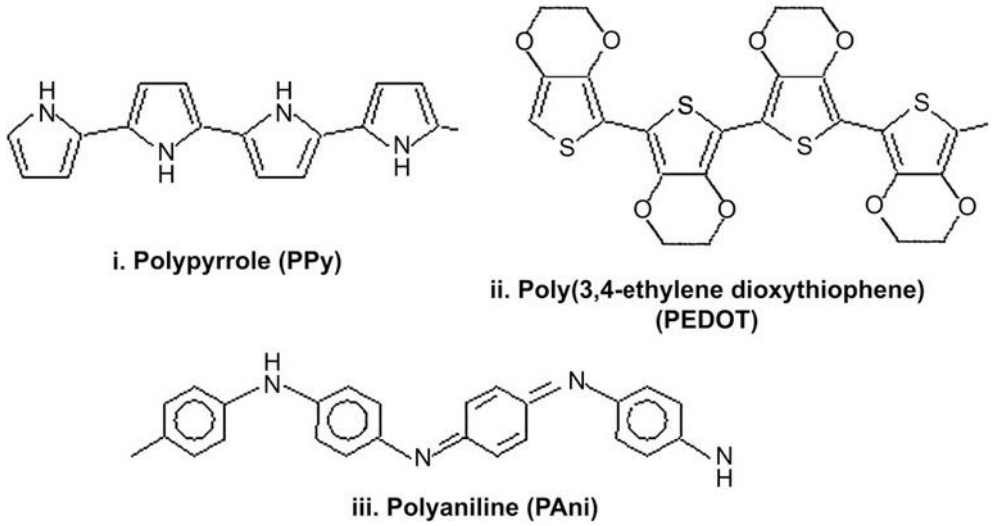

Figure 1.3: Structures of conducting polymers, (i) polypyrrole, (ii) poly(3,4-ethylene dioxythiophene), and (iii) polyaniline (Reprinted from Ref. [40], Copyright (2008) with permission from Elsevier).

Poly(3,4-ethylenedioxythiophene)(known as PEDOT) and its composite are also used in supercapacitor due to the properties such as low oxidation potential, high energy density from wider potential window (1.2-1.5 V), conducting p-doped state, thermal and chemical stability [42]. The high conductivity and surface area of PEDOT provides fast kinetics of PEDOT electrodes and exhibits longer cycle life. The chemical structures of PANI, PPy, and PEDOT are shown in Figure 1.3. But generally, conducting polymers show low cycling stability during rapid charge/discharge processes due to the swelling and shrinkage, results in mechanical degradation of the electrode material. For example, PPy electrode exhibits less than 50% of capacitive retention after 1000 cycles [43]. Polythiophene, another conducting polymer also shows poor cycling stability which minimizes the overall performance of ESs [42].

1.5 Graphene

The single layer of graphite is called Graphene. It is the most versatile electrode material known for supercapacitors. Graphene gains popularity as a 2D material after its discovery in the year of 2004 by Geim and Novoselov [44]. They prepared single layer of graphene using mechanical exfoliation (scotch-tap method). For this ground breaking discovery, they were awarded with Nobel Prize in Physics in the year 2010. The schematic diagram of graphene and graphene oxide are depicted in Figure 1.4. Graphene is popular for its light weight, tunable surface area (up to 2675 m^2g^{-1}), excellent electrical conductivity and mechanical strength (~1 TPa) [45, 46]. Graphene can also be used as a conductive network with transition metal oxides, conducting

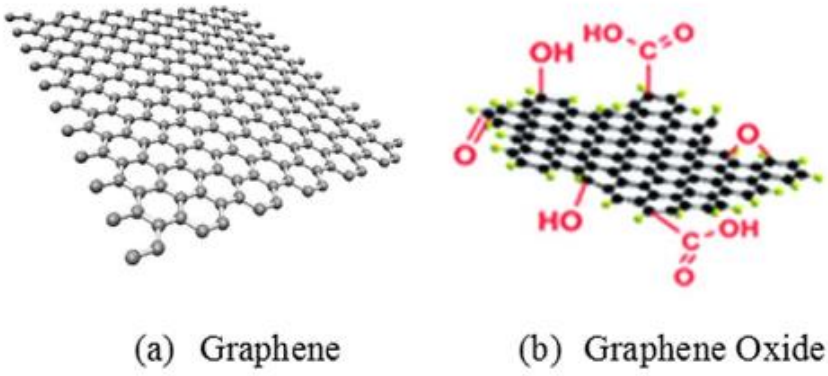

Figure 1.4: Schematic of graphene nanosheets and reduced graphene oxide, (Reprinted from Ref. [50], Copyright (2017) with permission from Elsevier).

polymer to assist the redox reactions and these hybrid composites exhibit enhanced electrochemical performances due to the synergetic effects of metal oxides/conducting polymers. The pioneered work by Ruoff et al. in the year of 2008, graphene was used for energy storage for the first time [47]. They developed chemically modified graphene as supercapacitor electrode and reported specific capacitance of 135 Fg^{-1} in aqueous electrolyte (KOH) and specific capacitance of 99 Fg^{-1} in nonaqueous electrolyte (tetraethylammonium tetrafluoroborate). Shi et al. reported one-step reduction process of GO and successfully prepared electrode material for supercapacitor with specific capacitance of 175 Fg^{-1} [48]. Graphene can be prepared with different morphologies by varying the dimension and used as an active material for supercapacitor electrodes. The different morphologies of graphene are (i) 0D graphene (free standing dots and

particles), (ii) 1D graphene (fiber-type),(iii) 2D graphene (graphene-based films and papers), and (iv) 3D graphene (graphene-based foams and hydrogels) [49]. The 0D graphene particles readily agglomerate and therefore it is essential to treat amphiphilic GO with selective surfactant to control the rGO assembly [50]. Zhanget al. investigated surfactant-assistant rGO film for supercapacitor and reported capacitance of 194 Fg^{-1} (1 Ag^{-1} of current density) [51]. Graphene material with yarn and fibrous morphology is gaining attention in the fabrication of next-generation supercapacitors due to the properties like high flexibility, great mechanical strength, tiny volume and great conductivity [52]. The 2D structure of graphene materials with larger surface area can offer easy intercalation/de-intercalation of electrolyte ions into the electrode materials. The great mechanical strength of graphene sheets helps to construct free standing films and its excellent conductivity minimizes the diffusion resistance leading to improved energy density, power density, and low electrode series resistance (ESR). The presence of all types of pores (micro, meso, and macropores) connected with each other in 3D porous graphene materials is desirable to fabricate supercapacitors with high capacity, enhanced energy, and power density [53-56]. The drawback associated with graphene is severe agglomeration during practical applications which reduces the electrochemical activity of such electrodes.

1.6 Molybdenum disulphide (MoS_2)

After graphene, research interests for 2D materials have refocused and there were enthusiasm among research community to find new materials analogous to graphene. One such example is Molybdenum Disulfide (MoS_2). It is a material in the category of Transition Metal Dichalcogenides (TMDCs). TMDCs is a family of large number of materials have generalized formulae MX_2 where M is transition metals (Ti, Pt, Ni, Co, Pd, Mo, Nb, W, Zr, Hf, V, Ta, Tc, Re, Rh, Ir) and X is Chalcogen (Te, Se, S) [57]. MoS_2 monolayer consists of a layer of molybdenum atoms sandwiched in two layers of sulphur atoms (S-Mo-S) (Figure 1.5). These monolayers are stacked together by weak van der Waals interaction and forms bulk MoS_2. In MoS_2, the Mo-S bond length is 1.54 Å and S-S bond is 3.08 Å. The layer thickness of MoS_2 is in general ~ 0.65 nm. Nanostructures of MoS_2 were synthesized either with top down method or bottom up approaches [58]. The top down methods includes electrochemical exfoliation, mechanical exfoliation and liquid phase exfoliation (ultra sound assisted, shear force

assisted). On the contrary, bottom up strategy deals with hydrothermal/solvothermal method, microwave synthesis and chemical vapor deposition methods for the development of MoS_2 nanostructures. These nanostructures found applications in energy storage because of the beneficial properties such as high catalytic activity, high surface area, and cycling stability [59, 60]. Central ion Mo in the sandwiched structure possesses various oxidation states from +4 to +6, providing pseudocapacitance for charge storage. In 2013, Cao et al. prepared micro supercapacitor with ten inter digitated electrodes of 2D MoS_2 [61]. These micro supercapacitors were reported stable enough with volumetric capacity of 178 Fcm^{-3} which is better than the other reported carbon based micro supercapacitors (~ 160 Fcm^{-3}). In 2018, Karade et al. reported supercapacitor electrodes prepared from ultrathin MoS_2 nanoflakes exhibiting specific capacitance of 576 Fg^{-1} in 0.5 M Na_2SO_4 [62]. These electrodes also possessed cycling stability of 82.2% after 3000 cycles. Nanocomposites of MoS_2 are also popular as energy storage active materials. Hu et al. synthesized porous tubular C/MoS_2 nanocomposites as electrode material for supercapacitors and obtained specific capacitance of 210 Fg^{-1} (1 Ag^{-1} current density) [63].

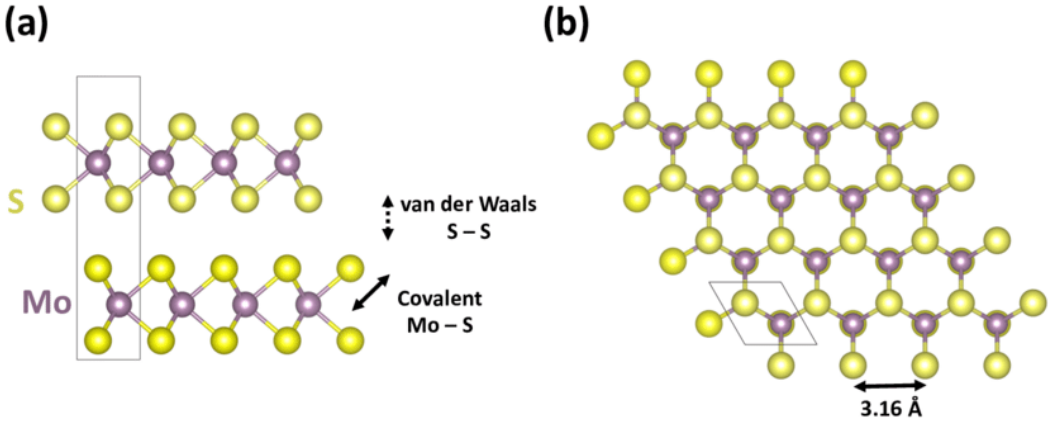

Figure 1.5: Crystal structure of MoS_2. (a) The layered MoS_2 crystal is held together by strong in-plane covalent Mo-S interactions and relatively weaker S-S van der Waals interactions. (b) The honeycomb crystal structure of MoS_2 has a lattice constant of 3.16 Å.

1.7 Swift heavy ion irradiation

Conducting polymers show poor cycling stability in repeated galvanostatic cycles as they undergo swelling and shrinkage. One of the novel techniques to stabilize the conducting polymers is swift heavy ion (SHI) irradiation. It is a renowned surface modification technique that can modify the physico-chemical properties of the target

by imparting electronic energy in a controlled way at the microscopic level [64]. Some well-known modifications by SHI irradiation on polymer are: intermolecular cross-linking, fragmentation of molecules, formation of new bond, bond breaking etc. The parameters on which SHI irradiation depends are (i) irradiation fluence and (ii) energy of the ion beam. The ion fluences of SHI irradiation can be calculated from the beam current and irradiation time according to the following equation:

$$Irradiation\ time(T) = \frac{\varphi \times A \times q \times e}{I} \qquad [1.1]$$

where φ is the fluence, A is the area exposed to ion beam, q is the charge state, e is electronic charge and I is current. In the process, energy deposition in the target material per unit length along ion track is energy loss written as dE/dx (eV/Å). Energy loss take place in two independent processes: (a) nuclear energy loss – the collision between the incident ions and the target nuclei is elastic in nature and dominating energy loss at about 1 keV/amu; (b) electronic energy loss – the collision between the incident ions and atomic electrons are inelastic in nature and dominating energy is around 1 MeV/amu or more. Energy is transferred to the target material through two independent processes depending upon the incident energy of the ions: (a) elastic collision at the target nuclei is nuclear energy loss $(dE/dx)_n$ at low incident energy(<1 MeV) and (b) inelastic collision at the electron cloud is electronic energy loss $(dE/dx)_e$ for high energy irradiation (>1 MeV) [65]. For SHI irradiation, inelastic collision is the dominant mechanism for energy transfer through ionization and excitation of the surrounding electrons. The interaction of the incident ions with the material is governed by two fundamental models: (a) coulomb explosion model and (b) thermal spike model [66]. According to the coulomb explosion model, a long cylinder containing ionized ions produced during the passage of SHI and explodes under Coulombic force [67]. Due to the radial Coulombic explosion of the cylindrical shock waves, ion tracks are formed along the ion trajectories. However, in thermal spike model, kinetic energy of the ejected electron during SHI is transferred to the lattice through electron-phonon interaction i.e. by defect formation, which increases the temperature of the local lattice beyond the melting point, followed by rapid quenching, which on solidification results in amorphous structures [68]. Conducting polymers are irradiation sensitive and many of its physico-chemical properties can be changed with this modification technique [69, 70].

1.8 MXene

MXene may be considered as a new member in the family of 2D materials after the first report on 2D titanium carbide (Ti_3C_2) in the year of 2011 by the group of Gogotsi [71]. MXenes are in general 2D transition metal carbides, nitrides, and carbonitrides with a common representation of $M_{n+1}X_nT_x$ (n=1-3), where M stands for transition metal such as Ti, Nb, Sc, V, Mo, Cr, X is nitrogen and/or carbon, T_x is terminal groups attached during exfoliation procedure. "MAX" is the ternary precursor of MXene where A typically stands for 13th and 14th group elements of periodic table such as, Al, In, Si, Ga etc. [72, 73]. MXenes are important due to tunable band gap, metallic conductivity, excellent mechanical properties, unique in-plane anisotropic structure etc. [74]. Because of these unique combinations of properties, MXenes could be used in diverse applications such as wearable and portable electronics, printable antennas, sensors, photocatalysis, fuel cell, biomedical activities, etc. [75-80]. However, the most extensive application of MXene is in the area of electrochemical energy storage systems.

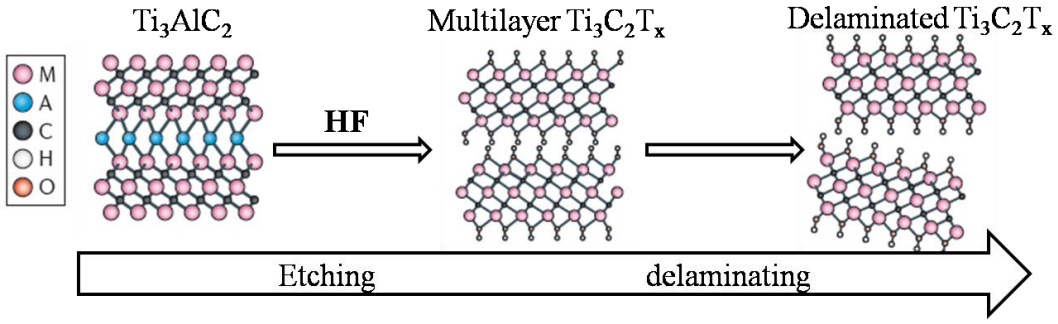

Figure 1.6: MAX phase (Ti_3AlC_2) to MXene ($Ti_3C_2T_x$). Layered ternary Ti_3AlC_2 MAX powder is treated with hydrofluoric acid (HF), then the Al layer is selectively etched and replaced with surface attached terminations groups (T_x), resulting in multilayered $Ti_3C_2T_x$ MXenes. Delaminated $Ti_3C_2T_x$ is prepared by the intercalation of solvent molecules and cations/anions into the interlayer spacing followed by ultrasoncation (Reprinted from Ref. [73], Copyright (2017) with permission from Springer Nature).

Unlike graphene, layers of MXenes are not attached with one another by van der Waals interaction force and, hence, the commonly used methods to obtain graphene monolayers are not applicable to synthesize 2D MXenes [74]. Typically, MXene could be derived from the precursors MAX phase by wet chemical top-down method [71]. This method is possible because of the higher chemical reactivity of M–A

bond than that of M–X bond. Therefore, selective etching of "A" layer from precursor MAX phase by using a suitable etching agent gives layered MXene. The separated layers of MXenes are look alike of graphene and due to this similarity; it was named as MXene [81]. These layered MXenes can be 1 nm thin and at the same time lateral size may be in microns. In general, Ti_3AlC_2 is treated with 50% of hydrofluoric acid (HF) for selective removal of Al (A layer) to obtain multilayered Ti_3C_2 followed by delaminating process to obtain 2D layered Ti_3C_2 nanosheets [76-79]. The schematic of the synthesis of MXenes from MAX phase is displayed in Figure 1.6. In this process, delaminated nanosheets are left with various surface functional groups like hydroxyl, and fluorine and these groups can regulate the properties of MXene [80]. Other than the use of direct HF acid, in-situ formation of HF, molten salts and ammonium hydrogen bifluoride (NH_4HF_2) have also been used by some of groups to prepare multilayered MXenes [72]. MXenes possess better properties than that of some of the 2D materials when comparing electrical conductivity. MXenes are considered for energy storage in batteries and supercapacitors owing to the following advantages : (i) 2D layered architecture provides easy access to more number of active sites for electrochemical reactions, (ii) high electrical conductivity which is necessary to provide shorter diffusion path for the charge carriers in the electrode, (iii) hydrophilic nature makes it convenient for dispersion in aqueous medium, (v) easy preparation of MXenes free-standing films, (vi) intercalation of different cations irrespective of size and charge state.

In the present thesis, Chapter 5 describes a novel HF free electrochemical method to obtain exfoliated MAX phase and also illustrates the Al^{3+}-ion storage in aqueous electrolyte.

1.9 Lithium Iron Phosphate ($LiFePO_4$)

Phosphate based olivine structures $LiMPO_4$ (M = Fe, Mn, Co, Ni) are also regarded as a notable cathode material in lithium-ion batteries [82]. The strong covalent bond P-O of the polyanion stabilizes these structures in a fully charged state. One example of olivine structures is $LiFePO_4$. It was first reported by Padhi et al. which is a notable discovery and it guides to set up a library of cathode materials for lithium-ion batteries [83]. $LiFePO_4$ has been extensively studied for non-aqueous lithium-ion batteries [84-88]. It attains a lot of research interest owing to its crystal structure, comparatively high

theoretical specific capacity (170 $mAhg^{-1}$), flat charge-discharge profiles, and better cycle life [88, 89]. Additionally, processing of $LiFePO_4$ involves inexpensive resources. It exhibits exceptionally flat charge-discharge profiles at a potential of 3.4 V (vs. Li^+/Li) with negligible polarization. Although the specific theoretical capacity of $LiFePO_4$ is less than $LiCoO_2$, one among the reasons why $LiFePO_4$ is a favorite cathode material for lithium-ion batteries is due to the possibility of replacement of toxic and scare cobalt with environment friendly and abundant iron species. In addition, the strong P-O covalent bond in $LiFePO_4$ impedes the release of oxygen which in turn provides intrinsic safety to the cell during any thermal runaway event [87]. The durability, thermal stability and calendar life of $LiFePO_4$ are magnificently impressive. But majority of the studies on $LiFePO_4$ was performed in non-aqueous electrolyte. There is only handful of reports on the aqueous Li^+-ion electrochemistry of $LiFePO_4$ for rechargeable aqueous batteries [89-91]. Manickam et al. first investigated the aqueous Li^+-ion electrochemistry of $LiFePO_4$ and it was shown in that study that oxidation and reduction of $LiFePO_4$ due to Li^+-ion extraction and insertion is possible in aqueous electrolyte [90]. While the usual Li^+-ion extraction takes place from $LiFePO_4$ during oxidation to form $FePO_4$, the reduction process involves formation of Fe_3O_4 along with $LiFePO_4$. This is certainly in contrast to the electrochemical reaction mechanism in non-aqueous electrolytes where $FePO_4$ transforms to the original state of $LiFePO_4$ during reduction [83, 92]. It was also revealed that the rate capability of $LiFePO_4$ is quite superior in aqueous electrolyte than non-aqueous electrolyte due to easier desolvation of Li^+-ion in aqueous electrolyte at the electrode-electrolyte interface [93, 94]. This reduction in interfacial charge transfer resistance was also observed by Sauvage et al. in their study on $LiFePO_4$ thin film electrode in aqueous system [95]. However, in general, the degree of specific capacity fading is much higher in aqueous electrolyte than non-aqueous electrolyte due to the electrochemical instability of $LiFePO_4$ in aqueous electrolyte, which could be significantly mitigated by adopting strategies such as nanoscopic carbon coating of $LiFePO_4$ [96]. Additionally, CeO_2 coating and doping of $LiFePO_4$ also improves the stability [94, 97].

In the present thesis, Chapter 6 illustrates the Al^{3+}-ion storage electrochemistry for $LiFePO_4$ in aqueous electrolyte which is hitherto been unknown.

1.10 References

[1] https://www.iea.org/reports/world-energy-outlook-2021/executive-summary.

[2] https://www.energy.gov/sites/default/files/2022-05/41001%20RFI%205.2.22_EOP_v2%20CLEAN%20No%20Watermark%20PDF.pdf.

[3] https://www.gov.uk/government.

[4] Purkait, T., Singh, G., Kumar, D., Singh, M., and Dey, R. S. High-performance flexible supercapacitors based on electrochemically tailored three-dimensional reduced graphene oxide networks. *Scientific reports*, 8(1): 640, 2018.

[5] Chiam, S. L., Lim, H. N., Hafiz, S. M., Pandikumar, A., and Huang, N. M. Electrochemical performance of supercapacitor with stacked copper foils coated with graphene nanoplatelets. *Scientific reports*, 8(1): 1-7, 2018.

[6] Zhou, Y., Jin, P., Zhou, Y., and Zhu, Y. High-performance symmetric supercapacitors based on carbon nanotube/graphite nanofiber nanocomposites. *Scientific reports*, 8(1): 1-7, 2018.

[7] Becker, H. I. Low voltage electrolytic capacitor. U.S. Patent 2,800,616, issued July 23, 1957.

[8] Wang, D. W., Fang, H. T., Li, F., Chen, Z. G., Zhong, Q. S., Lu, G. Q., and Cheng, H. M. Aligned titania nanotubes as an intercalation anode material for hybrid electrochemical energy storage. *Advanced Functional Materials*, 18(23): 3787-3793, 2008.

[9] Zuo, X., and Jin, Z., Müller-Buschbaum, P., and Cheng, Y. J. Silicon based lithium-ion battery anodes: A chronicle perspective review. *Nano Energy*, 31: 113-143, 2017.

[10] Chen, D., Zheng, F., Li, L., Chen, M., Zhong, X., Li, W., and Lu, L. Effect of Li3PO4 coating of layered lithium-rich oxide on electrochemical performance. *Journal of Power Sources*, 341: 147-155, 2017.

[11] Helmholtz, V. H. On the conservation of force. *Annals of Physics (Leipzig)*, 89: 21, 1853.

[12] Stern, O. The theory of the electrolytic double-layer. *Z. Elektrochem*, 30(508): 1014-1020, 1924.

[13] Grahame, D. C. The electrical double layer and the theory of electrocapillarity. *Chemical reviews*, 41(3): 441-501, 1947.

[14] Zhang, L., Zhang, T. D., Gao, R., Tang, D. Y., Tang, J. Y., and Zhan, Z. L. Preparation and Characterization of Mesoporous Carbon Materials of Chinese Medicine Residue with High Specific Surface Areas. *Chemical Engineering Transactions*, 55: 79-84, 2016.

[15] Kötz, R., Hahn, M., and Gallay, R. Temperature behavior and impedance fundamentals of supercapacitors. *Journal of Power Sources*, 154(2): 550-555, 2006.

[16] Burke, A. R&D considerations for the performance and application of electrochemical capacitors. *Electrochimica Acta*, 53(3): 1083-1091, 2007.

[17] Zhu, Y., Ji, X., Pan, C., Sun, Q., Song, W., Fang, L., Chen, Q., and Banks, C. E. A carbon quantum dot decorated RuO_2 network: outstanding supercapacitances under ultrafast charge and discharge. *Energy & Environmental Science*, 6(12): 3665-3675, 2013.

[18] Wayu, M. Manganese oxide carbon-based nanocomposite in energy storage applications. *Solids*, 2(2): 232-248, 2021.

[19] Goodenough, J. B., and Kyu-Sung P. The Li-ion rechargeable battery: a perspective. *Journal of the American Chemical Society*, 135(4): 1167-1176, 2013.

[20] Barreras, J. V., Cláudio P., Ricardo de C., Erik S., Soren J. A., and Rui E. A. Multi-objective control of balancing systems for li-ion battery packs: A paradigm shift?. *In IEEE Vehicle Power and Propulsion Conference (VPPC)*, pp. 1-7, 2014.

[21] Goodenough, J. B. How we made the Li-ion rechargeable battery. *Nature Electronics*, 1 (3): 204-204, 2018.

[22] Peters, J. F., Manuel B., Benedikt Z., Jessica B., and Marcel W. The environmental impact of Li-Ion batteries and the role of key parameters–A review. *Renewable and Sustainable Energy Reviews*, 67: 491-506, 2017.

[23] Holleck, G. L. The Reduction of Chlorine on Carbon in AlCl3-KCl-NaCl Melts. *Journal of Electrochemical Society*, 119(9): 1158-1161, 1972.

[24] Holleck, G. L., and Giner, J. The Aluminum Electrode in AlCl3-Alkali-Halide Melts. *Journal of Electrochemical Society*, 119(9): 1161-1166, 1972.

[25] Jayaprakash, N., Das, S. K., and Archer, L. A. The rechargeable aluminum-ion battery. *Chemical Communications*, 47: 12610-12612, 2011.

[26] Lin, M.C., Gong, M., Lu, B., Wu, Y., Wang, D.Y., Guan, M., Angell, M., Chen, C., Yang, J., Hwang, B.J., and Dai, H. An ultrafast rechargeable aluminium-ion battery. *Nature*, 520 (7547): 324-328, 2015.

[27] Li, W., McKinnon, W. R., and Dahn, J. R. Lithium intercalation from aqueous solutions. *Journal of the Electrochemical Society*, 141(9): p.2310, 1994.

[28] Liu, S., Pan, G.L., Li, G.R., and Gao, X.P. Copper hexacyanoferrate nanoparticles as cathode material for aqueous Al-ion batteries. *Journal of Materials Chemistry A*, 3(3): pp.959-962, 2015.

[29] Liu, S., Hu, J. J., Yan, N. F., Pan, G. L., Li, G. R., and Gao, X. P. Aluminum storage behavior of anatase TiO_2 nanotube arrays in aqueous solution for aluminum ion batteries. *Energy & Environmental Science*, 5(12): 9743-9746, 2012.

[30] Kazazi, M., Abdollahi, P., and Mirzaei-Moghadam, M. High surface area TiO2 nanospheres as a high-rate anode material for aqueous aluminum-ion batteries. *Solid State Ionics*, 300: 32-37, 2017.

[31] Liu, Y., Sang, S., Wu, Q., Lu, Z., Liu, K., and Liu, H. The electrochemical behavior of Cl^- assisted Al^{3+} insertion into titanium dioxide nanotube arrays in aqueous solution for aluminum ion batteries. *Electrochimica Acta*, 143: 340-346, 2014.

[32] Lahan, H., Boruah, R., Hazarika, A, and Das, S. K. Anatase TiO2 as an anode material for rechargeable aqueous aluminum-ion batteries: remarkable graphene induced aluminum ion storage phenomenon. *The Journal of Physical Chemistry C*, 121(47): 26241-26249, 2017.

[33] Lahan, H., and Das, S. K. Al^{3+} ion intercalation in MoO3 for aqueous aluminum-ion battery. *Journal of Power Sources*, 413: 134-138, 2019.

[34] Lahan, H., and Das, S. K. Reversible Al^{3+} ion insertion into tungsten trioxide (WO 3) for aqueous aluminum-ion batteries. *Dalton Transactions*, 48(19): 6337-6340, 2019.

[35] Shi, Y., Peng, L., Ding, Y., Zhao, Y., and Yu, G. Nanostructured conductive polymers for advanced energy storage. *Chemical Society Reviews*, *44*(19): 6684-6696, 2015.

[36] Green, R. A., Lovell, N. H., Wallace, G. G., and Poole-Warren, L. A. Conducting polymers for neural interfaces: challenges in developing an effective long-term implant. *Biomaterials*, 29(24-25): 3393-3399, 2008.

[37] Eftekhari, A., Li, L., and Yang, Y. Polyaniline supercapacitors. *Journal of Power Sources*, 347: 86-107, 2017.

[38] Ryu, K. S., Kim, K. M., Park, N. G., Park, Y. J., and Chang, S. H. Symmetric redox supercapacitor with conducting polyaniline electrodes. *Journal of Power Sources*, 103(2): 305-309, 2002.

[39] Talbi, H., Just, P. E., and Dao, L. H. Electropolymerization of aniline on carbonized polyacrylonitrile aerogel electrodes: applications for supercapacitors. *Journal of Applied Electrochemistry*, 33(6): 465-473, 2003.

[40] Ryu, K. S., Kim, K. M., Park, Y. J., Park, N. G., Kang, M. G., and Chang, S. H. Redox supercapacitor using polyaniline doped with Li salt as electrode. *Solid State Ionics*, 152: 861-866, 2002.

[41] Ko, J. M., Rhee, H. W., Park, S.M., and Kim, C. Y. Morphology and Electrochemical Properties of Polypyrrole Films Prepared in Aqueous and Nonaqueous Solvents. *Journal of Electrochemical Society*, 137(3): 905-909, 1990.

[42] Fu, C., Zhou, H., Liu, R., Huang, Z., Chen, J., and Kuang, Y. Supercapacitor based on electropolymerized polythiophene and multi-walled carbon nanotubes composites. *Materials Chemistry and Physics*, 132(2-3): 596-600, 2012.

[43] Song, Y., Liu, T.Y., Xu, X.X., Feng, D.Y., Li, Y. and Liu, X.X. Pushing the cycling stability limit of polypyrrole for supercapacitors. *Advanced Functional Materials*, 25(29): 4626-4632, 2015.

[44] Novoselov, K. S., Geim, A. K., Morozov, S. V., Jiang, D., Zhang, Y., Dubonos, S. V., Grigorieva, I. V., and Firsov, A. A. Electric field effect in atomically thin carbon films. *Science*, 306(5696): 666-669, 2004.

[45] Lee, C., Wei, X., Kysar, J. W., and Hone, J. Measurement of the elastic properties and intrinsic strength of monolayer graphene. *Science*, 321(5887): 385-388, 2008.

[46] Li, X., and Zhu, H. Two-dimensional MoS2: Properties, preparation, and applications. *Journal of Materiomics*, 1(1): 33-44, 2015.

[47] Stoller, M. D., Park, S., Zhu, Y., An, J., and Ruoff, R. S. Graphene-based ultracapacitors. *Nano letters*, 8(10): 3498-3502, 2008.

[48] Shi, W., Zhu, J., Sim, D. H., Tay, Y. Y. , Lu, Z., Zhang, X., Sharma, Y., Srinivasan, M., Zhang, H., Hng, H.H. and Yan, Q. Achieving high specific charge capacitances in Fe_3O_4/reduced graphene oxide nanocomposites. *Journal of Materials Chemistry*, 21(10): 3422-3427, 2011.

[49] Ke, Q., and Wang, J. Graphene-based materials for supercapacitor electrodes–A review. *Journal of Materiomics*, 2(1): 37-54, 2016.

[50] Byon, H. R., Lee, S. W., Chen, S., Hammond, P. T., and Shao-Horn, Y. Thin films of carbon nanotubes and chemically reduced graphenes for electrochemical micro-capacitors. *Carbon*, 49(2): 457-467, 2011.

[51] Zhang, K., Mao, L., Zhang, L. L., Chan, H. S. O., Zhao, X. S., and Wu, J. Surfactant-intercalated, chemically reduced graphene oxide for high performance supercapacitor electrodes. *Journal of Materials Chemistry*, 21(20): 7302-7307, 2011.

[52] Meng, Y., Zhao, Y., Hu, C., Cheng, H., Hu, Y., Zhang, Z., Shi, G., and Qu, L. All-graphene core-sheath microfibers for all solid state, stretchable fibriform supercapacitors and wearable electronic textiles. *Advanced materials*, 25(16): 2326-2331, 2013.

[53] Chen, H., Müller, M. B., Gilmore, K. J., Wallace, G. G., and Li, D. Mechanically strong, electrically conductive, and biocompatible graphene paper. *Advanced Materials*, 20(18): 3557-3561, 2008.

[54] Tung, V. C., Kim, J., Cote, L. J., and Huang, J. Sticky interconnect for solution-processed tandem solar cells. *Journal of the American Chemical Society*, 133(24): 9262-9265, 2011.

[55] Liu, F., and Seo, T. S. A controllable self-assembly method for large-scale synthesis of graphene sponges and free-standing graphene films. *Advanced Functional Materials*, 20(12): 1930-1936, 2010.

[56] Yin, S., Zhang, Y., Kong, J., Zou, C., Li, C. M., Lu, X., Ma, J., Boey, F. Y. C., and Chen, X. Assembly of graphene sheets into hierarchical structures for high-performance energy storage. *Acs Nano*, 5(5): 3831-3838, 2011.

[57] Arshad, M. K. Md, Gopinath, S. CB., Norhaimi, W. M. W., and Fathil, M. F. M. Current and future envision on developing biosensors aided by 2D

molybdenum disulfide (MoS_2) productions. *Biosensors and Bioelectronics*, 132: 248-264, 2019.

[58] Abdel Maksoud, M.I.A., Bedir, A.G., Bekhit, M., Abouelela, M.M., Fahim, R.A., Awed, A.S., Attia, S.Y., Kassem, S.M., Elkodous, M.A., El-Sayyad, G.S. and Mohamed, S.G. MoS_2-based nanocomposites: synthesis, structure, and applications in water remediation and energy storage: a review. *Environmental Chemistry Letters*, *19*(5):3645-3681, 2021.

[59] Wang, Y.X., Seng, K.H., Chou, S.L., Wang, J.Z., Guo, Z., Wexler, D., Liu, H.K., and Dou, S.X. Reversible sodium storage via conversion reaction of a MoS_2–C composite. *Chemical Communications*, 50(73): 10730-10733, 2014.

[60] Lin, Z., Carvalho, B.R., Kahn, E., Lv, R., Rao, R., Terrones, H., Pimenta, M.A. and Terrones, M. Defect engineering of two-dimensional transition metal dichalcogenides. *2D Materials*, 3(2): 022002, 2016.

[61] Cao, L., Yang, S., Gao, W., Liu, Z., Gong, Y., Ma, L., Shi, G., Lei, S., Zhang, Y., Zhang, S. and Vajtai, R. Direct laser-patterned micro-supercapacitors from paintable MoS_2 films. *Small*, 9(17): 2905-2910, 2013.

[62] Karade, S. S., Dubal, D. P., and Sankapal, B. R. MoS 2 ultrathin nanoflakes for high performance supercapacitors: room temperature chemical bath deposition (CBD). *RSC advances*, 6(45): 39159-39165, 2016.

[63] Hu, B., Qin, X., Asiri, A. M., Alamry, K. A., Al-Youbi, A. O., and Sun, X. Synthesis of porous tubular C/MoS_2 nanocomposites and their application as a novel electrode material for supercapacitors with excellent cycling stability. *Electrochimica Acta*, 100: 24-28, 2013.

[64] Balanzat, E., Bouffard, S., Le Moël, A., and Betz, N. Physico-chemical modifications induced in polymers by swift heavy ions. *Nuclear Instruments and Methods in Physics Research Section B: Beam Interactions with Materials and Atoms*, 91(1-4): 140-145, 1994.

[65] Avasthi, D. K. Some interesting aspects of swift heavy ions in materials science. *Current Science*, 78(11): 1297-1303, 2000.

[66] Bringa, E. M., and Johnson, R. E. Coulomb Explosion and Thermal Spikes. *Physical Review Letters*, 88: 16, 2002.

[67] Last, I., Schek, I., and Jortner, J. Energetics and dynamics of Coulomb explosion of highly charged clusters. *The Journal of Chemical Physics*, 107(17): 6685-6692, 1997.

[68] Szenes, G. Thermal spike model of amorphous track formation in insulators irradiated by swift heavy ions. *Nuclear Instruments and Methods in Physics Research B*, 116: 141-144, 1996.

[69] Hussain, A.M.P., Kumar, A., Singh, F., and Avasthi, D. K. Effects of 160 MeV Ni^{12+} ion irradiation on HCl doped polyaniline electrode. *Journal of Physics D: Applied Physices*, 39: 750–755, 2006.

[70] Sarmah, S., and Kumar, A. SHI irradiation effects on electrical and optical properties of PPy–SnO_2 nanocomposite. *Physica Status Solidi A*, 207(10): 2279–2287, 2010.

[71] Naguib, M., Kurtoglu, M., Presser, V., Lu, J., Niu, J., Heon, M., Hultman, L., Gogotsi, Y., and Barsoum, M. W. Two dimensional nanocrystals produced by exfoliation of Ti_3AlC_2. *Advanced materials*, 23(37): 4248-4253, 2011.

[72] Gogotsi, Y., and Anasori, B. The rise of MXenes. *ACS Nano*, 13: 8491–8494, 2019.

[73] Zhang, C., Ma, Y., Zhang, X., Abdolhosseinzadeh, S., Sheng, H., Lan, W., Pakdel, A., Heier, J., and Nüesch, F. Two dimensional transition metal carbides and nitrides (MXenes): synthesis, properties, and electrochemical energy storage applications. *Energy & Environmental Materials*, 3(1): 29-55, 2020.

[74] Lei, J. C., Zhang, X., and Zhou, Z. Recent advances in MXene: Preparation, properties, and applications. *Frontiers of Physics*, 10(3): 276-286, 2015.

[75] Rasool, K., Helal, M., Ali, A., Ren, C. E., Gogotsi, Y., and Mahmoud, K. A. Antibacterial activity of $Ti_3C_2T_x$ MXene. *ACS nano*, 10(3): 3674-3684, 2016.

[76] Tang, Q., Zhou, Z., and Shen, P. Are MXenes promising anode materials for Li ion batteries? Computational studies on electronic properties and Li storage capability of Ti_3C_2 and $Ti_3C_2X_2$ (X= F, OH) monolayer. *Journal of the American Chemical Society*, 134(40): 16909-16916, 2012.

[77] Hu, T., Hu, M., Li, Z., Zhang, H., Zhang, C., Wang, J., and Wang, X. Covalency-dependent vibrational dynamics in two-dimensional titanium carbides. *The Journal of Physical Chemistry A*, 119(52): 12977-12984, 2015.

[78] Han, M., Liu, Y., Rakhmanov, R., Israel, C., Tajin, Md. A. S., Friedman, G., Volman, V., Hoorfar, A., Dandekar, K. R., and Gogotsi, Y. Solution-processed Ti3C2Tx MXene antennas for radio-frequency communication. *Advanced Materials*, 33(1): 2003225, 2021.

[79] Li, K., Liang, M., Wang, H., Wang, X., Huang, Y., Coelho, J., Pinilla, S., Zhang, Y., Qi, F., Nicolosi, V. and Xu, Y. 3D MXene architectures for efficient energy storage and conversion. *Advanced Functional Materials*, 30(47): 2000842, 2020.

[80] Naguib, M., Mashtalir, O., Carle, J., Presser, V., Lu, J., Hultman, L., Gogotsi, Y., and Barsoum, M. W. Two-dimensional transition metal carbides. *ACS nano*, 6(2): 1322-1331, 2012.

[81] Naguib, M., Halim, J., Lu, J., Cook, K. M., Hultman, L., Gogotsi, Y., and Barsoum, M. W. New two-dimensional niobium and vanadium carbides as promising materials for Li-ion batteries. *Journal of the American Chemical Society*, 135(43): 15966-15969, 2013.

[82] Yonemura, M., Yamada, A., Takei, Y., Sonoyama, N., and Kanno, R. Comparative kinetic study of olivine Li_xMPO_4 (M= Fe, Mn). *Journal of the Electrochemical Society*, 151(9): A1352, 2004.

[83] Padhi, A. K., Nanjundaswamy, K. S., and Goodenough, J. B., Phospho olivines as positive electrode materials for rechargeable lithium batteries. *Journal of the electrochemical society*, 144(4): 1188, 1997.

[84] Padhi, A. K., Nanjundaswamy, K. S., Masquelier, C., Okada, S., and Goodenough, J. B. Effect of structure on the Fe^{3+}/Fe^{2+} redox couple in iron phosphates. *Journal of the Electrochemical Society*, 144(5): 1609, 1997.

[85] Reklaitis, J., Davidonis, R., Dindune, A., Valdniece, D., Jasulaitienė, V., and Baltrūnas, D. Characterization of LiFePO4/C composite and its thermal stability by Mössbauer and XPS spectroscopy. *physica status solidi (b)*, 253(11): 2283-2288, 2016.

[86] He, P., Zhang, X., Wang, Y. G., Cheng, L., and Xia, Y. Y. Lithium-ion intercalation behavior of $LiFePO_4$ in aqueous and nonaqueous electrolyte solutions. *Journal of the Electrochemical Society*, 155(2): A144, 2007.

[87] Zaghib, K., Dubé, J., Dallaire, A., Galoustov, K., Guerfi, A., Ramanathan, M., Benmayza, A., Prakash, J., Mauger, A., and Julien, C. M. Enhanced thermal

safety and high power performance of carbon-coated $LiFePO_4$ olivine cathode for Li-ion batteries. *Journal of Power Sources*, 219: 36-44, 2012.

[88] Takahashi, M., Ohtsuka, H., Akuto, K., and Sakurai, Y. Confirmation of long-term cyclability and high thermal stability of $LiFePO_4$ in prismatic lithium-ion cells. *Journal of the Electrochemical Society*, 152(5): A899, 2005.

[89] Sauvage, F., Tarascon, J-M., and Baudrin, E. Insights into the potentiometric response behaviour vs. Li^+ of $LiFePO_4$ thin films in aqueous medium. *Analytica chimica acta*, 622(1-2): 163-168, 2008.

[90] Manickam, M., Singh, P., Thurgate, S., and Prince, K. Redox behavior and surface characterization of $LiFePO_4$ in lithium hydroxide electrolyte. *Journal of power sources*, 158(1): 646-649, 2006.

[91] Noerochim, L., Yurwendra, A. O., and Susanti, D. Effect of carbon coating on the electrochemical performance of $LiFePO_4$/C as cathode materials for aqueous electrolyte lithium-ion battery. *Ionics*, 22(3): 341-346, 2016.

[92] Love, C. T., Korovina, A., Patridge, C. J., Swider-Lyons, K. E., Twigg, M. E., and Ramaker, D. E. Review of $LiFePO_4$ phase transition mechanisms and new observations from x-ray absorption spectroscopy. *Journal of The Electrochemical Society*, 160(5): A3153, 2013.

[93] He, P., Zhang, X., Wang, Y. G., Cheng, L., and Xia, Y.Y. Lithium-ion intercalation behavior of $LiFePO_4$ in aqueous and nonaqueous electrolyte solutions. *Journal of the Electrochemical Society*, 155(2): A144, 2007.

[94] Liu, X. H., Saito, T., Doi, T., Okada, S., and Yamaki, J. Electrochemical properties of rechargeable aqueous lithium ion batteries with an olivine-type cathode and a Nasicon-type anode. *Journal of Power Sources*, 189(1): 706-710, 2009.

[95] Sauvage, F., Laffont, L., Tarascon, J.M., and Baudrin, E. Factors affecting the electrochemical reactivity vs. lithium of carbon-free $LiFePO_4$ thin films. *Journal of Power Sources*, 175(1): 495-501, 2008.

[96] He, P., Liu, J.L., Cui, W.J., Luo, J.Y., and Xia, Y.Y. Investigation on capacity fading of $LiFePO_4$ in aqueous electrolyte. *Electrochimica acta*, 56(5): 2351-2357, 2011.

[97] Liu, Y., Mi, C., Yuan, C., and Zhang, X. Improvement of electrochemical and thermal stability of $LiFePO_4$ cathode modified by CeO_2. *Journal of Electroanalytical Chemistry*, 628(1-2): 73-80, 2009.